RSC Advances

PAPER

View Article Online
View Journal | View Issue

Cite this: *RSC Adv.*, 2017, **7**, 6809

Spinel $MgAl_2O_4$ modification on $LiCoO_2$ cathode materials with the combined advantages of MgO and Al_2O_3 modifications for high-voltage lithium-ion batteries†

D. D. Liang,[a] H. F. Xiang,*[a] X. Liang,[a] S. Cheng[c] and C. H. Chen[b]

In order to improve the electrochemical performance of $LiCoO_2$ cathode in a high-voltage range of 3.0–4.5 V, spinel $MgAl_2O_4$ has been modified on the surface of $LiCoO_2$ particle by a facile high-temperature solid state reaction. The structure and morphology of the $MgAl_2O_4$-modified $LiCoO_2$ are investigated in comparison with the pristine, Al_2O_3-modified and MgO-modified $LiCoO_2$. The $MgAl_2O_4$ modification is highly conformal and uniform just similar as the Al_2O_3 modification, while the MgO modification is not uniform. In terms of electrochemical performance as a high-voltage cathode material, the $MgAl_2O_4$-modified $LiCoO_2$ delivers an initial discharge capacity of 184 mA h g^{-1} between 3.0 V and 4.5 V at 0.1C (1C-rate = 160 mA g^{-1}) and a capacity retention of 96.8% after 70 cycles at 1C rate. There is a significant improvement on high-voltage cycling stability for the $MgAl_2O_4$-modified $LiCoO_2$ since the capacity retention of the pristine $LiCoO_2$ is only 38.7% after 70 cycles. Moreover, the $MgAl_2O_4$-modified $LiCoO_2$ exhibits an enhanced rate capability. Compared with the Al_2O_3 modification and the MgO modification, spinel $MgAl_2O_4$ modification has the combined advantages of Al_2O_3 and MgO modifications on improving the electrochemical performance of the $LiCoO_2$ cathode for high-voltage applications. The modified spinel $MgAl_2O_4$ layer can effectively protect the charged $Li_{1-x}CoO_2$ cathode from structural collapse and impede the oxidation decomposition of the electrolyte for the high-voltage application of $LiCoO_2$.

Received 28th November 2016
Accepted 9th January 2017

DOI: 10.1039/c6ra27463c

www.rsc.org/advances

Introduction

Lithium (Li) ion batteries composed of a $LiCoO_2$ cathode and a graphite anode are the dominating power sources for commercial 3C electronic devices at present. In order to extend the endurance of devices, the capacity of $LiCoO_2$ cathode as the capacity-limited component in the batteries must been enhanced. Theoretically, $LiCoO_2$ can deliver a capacity of 274 mA h g^{-1} after entire lithium ions extract out.[1] Nevertheless, its practical capacity is usually limited to only 137 mA h g^{-1} corresponding to $Li_{1-x}CoO_2$ ($x = 0.5$) with the cut-off voltage of 4.2 V in order to maintain the good structure stability and compatibility with nonaqueous electrolyte. A higher specific capacity can be gained by charging to a high voltage over 4.2 V, but worse cycling stability need be overcome. At higher voltages than 4.2 V, serious side reactions between the charged $Li_{1-x}CoO_2$ ($1 > x > 0.5$) cathode and nonaqueous electrolyte components cause the structural collapse of $Li_{1-x}CoO_2$ cathode and the serious oxidative decomposition of the electrolyte.[2,3]

To achieve the high-voltage application of $LiCoO_2$, many efforts have been made by either electrolyte reformulation or $LiCoO_2$ modification. Surface modification with metal oxides (*e.g.*, Al_2O_3,[4–7] MgO,[8,9] ZrO_2 (ref. 10 and 11)) has been widely reported as a facile and effective way to the high-voltage application of $LiCoO_2$ cathode materials. It is reported that a "zero-strain" $LiCoO_2$ cathode can be obtained by the surface modification with a thin layer of a high-fracture-toughness metal oxides, which can suppress the lattice constant changes and phase transitions of $LiCoO_2$ during high-voltage cycling.[12,13] Most recently, it is proposed that the surface modification could lead to improvement of the structural stability at the surface region of $LiCoO_2$.[14] Moreover, the modified layer can provide a physical barrier to suppress the interfacial side reactions between the charged $LiCoO_2$ and the electrolyte, which is also important for stabilizing the $LiCoO_2$ surface.[15] Therefore, the crystal structure and conductivity of the modified materials, the

[a]*School of Materials Science and Engineering, Hefei University of Technology, Hefei, Anhui, 230009, PR China. E-mail: hfxiang@hfut.edu.cn; Fax: +86-551-62901362; Tel: +86-551-62901457*

[b]*CAS Key Laboratory of Materials for Energy Conversions, Department of Materials Science and Engineering, University of Science and Technology of China, Hefei, Anhui 230026, China*

[c]*Instrumental Analysis Center, Hefei University of Technology, Hefei, Anhui 230009, PR China*

† Electronic supplementary information (ESI) available. See DOI: 10.1039/c6ra27463c

coverage ratio of the modified layer on $LiCoO_2$ are very important to modify the $LiCoO_2$ cathode materials for high-voltage Li-ion batteries. Recently, modification with Li^+-ion conductors on high-voltage cathode materials has attracted greater interests because of the advantageous combination of both physical barrier and Li^+-ion conduction.[16–18]

Both Al_2O_3 and MgO modified layers have been demonstrated to improve the cycling stability of $LiCoO_2$ at a high-voltage range. It was previously reported that Al_2O_3 modification inhibited the volume change of the $LiCoO_2$ lattice,[4] and MgO modification provided Mg^{2+} ions as pillars to stabilize the layered structure of $Li_{1-x}CoO_2$ ($1 > x > 0.5$) by diffusing into Co and Li sites during heat treatment.[8] Seldom literatures reported the effect of Al_2O_3 and MgO co-modification on the electrochemical performance of $LiCoO_2$ cathode in a high-voltage range. Recently, spinel $MgAl_2O_4$ has been incorporated into the cathode composite materials and solid electrolytes as a promising Li^+ ion conductor for applications in Li-ion batteries.[19–23] In this work, we investigate the effect of spinel $MgAl_2O_4$ modification on $LiCoO_2$ cathode by comparison with Al_2O_3 and MgO modifications. Our results show that spinel $MgAl_2O_4$ modification has combined advantages of Al_2O_3 and MgO modifications on improving the electrochemical performance of the $LiCoO_2$ cathode for high-voltage applications.

Experimental

Materials synthesis

All the starting materials were purchased from commercial sources and used without further purification. Commercial $LiCoO_2$ powders were obtained from Chinese company as the pristine and used for surface modification. To prepare $MgAl_2O_4$-modified $LiCoO_2$ powders, the $LiCoO_2$ powders were dispersed into distilled water. Then, $Al(NO_3)_3 \cdot 9H_2O$ and $Mg(NO_3)_2 \cdot 6H_2O$ with the molar ratio of 2 : 1 were poured into the solution. The mass ratio of $LiCoO_2$ *versus* the final received $MgAl_2O_4$ was controlled to be 99 : 1. After stirring for 10 min, 2% $NH_3 \cdot H_2O$ solution was dropped into the solution to adjust pH value to 8. After stirring for another 1 h, the suspension was dried at 60 °C and 120 °C to receive dry powders. The $MgAl_2O_4$-modified $LiCoO_2$ powders were finally obtained after heat-treatment at 800 °C for 6 h in air. For comparison, the Al_2O_3, MgO-modified $LiCoO_2$ powders were prepared at a similar procedure. The mass of the modified Al_2O_3 and MgO was controlled to be 1% of the final products. Herein, the content of 1% is the optimal in terms of the electrochemical performance.

Physical characterization

The crystal structures of the pristine $LiCoO_2$, $MgAl_2O_4$, Al_2O_3 and MgO-modified $LiCoO_2$ samples were characterized by X-ray diffraction (XRD) using a diffractometer (D/MAX2500 V, Cu Kα radiation). The XRD patterns were recorded from 10° to 70° (2 theta), and an internal standard of silicon powders were used to confirm the peak shifts. Rietveld refinement of 1% $MgAl_2O_4$-modified $LiCoO_2$ was carried out by using GSAS software. Morphologies of the pristine $LiCoO_2$ and Al_2O_3, MgO, $MgAl_2O_4$-modified $LiCoO_2$ were observed by field-emission scanning electron microscopy (FE-SEM, Hitachi SU8020) and high resolution transmission electron microscopy (HRTEM, JEM-2100F). X-ray photoelectron spectroscopy (XPS, ESCALAB250) was used to characterize the surface state of various $LiCoO_2$ powders, and the depth profiles of Al and Mg in the 1% $MgAl_2O_4$-modified $LiCoO_2$ were analysed on the electron spectroscopy for chemical analysis (ESCA) instrument (ESCALAB250).

Electrochemical measurement

The electrochemical properties of various $LiCoO_2$ cathode materials were evaluated in Li||$LiCoO_2$ CR2032-type coin cells. The $LiCoO_2$ electrodes for the coin cell assembly are prepared as follows: (1) a slurry containing $LiCoO_2$ material with or without modification, acetylene black, and polyvinylidene fluoride (PVDF) with the mass ratio of 84 : 8 : 8 was formed in *N*-methyl-2-pyrrolidinone (NMP); (2) the slurry was cast onto an aluminum current collector with a controlled thickness; (3) a $LiCoO_2$ laminate was received after NMP removal by vacuum drying at 70 °C; (4) the laminate was punched into discs (Φ 14 mm) as the $LiCoO_2$ electrodes. Microporous polypropylene membrane was used as separator. Highly pure lithium foil was used as the counter electrode and reference electrode in the Li||$LiCoO_2$ coin cell. The electrolyte was 1 M $LiPF_6$/ethylene carbonate (EC) + ethyl methyl carbonate (DMC) (1 : 1 w/w). The coin cells using various $LiCoO_2$ electrodes were assembled in an Ar-filled glove box (MBraun). The cell performance of the Li||$LiCoO_2$ cells using the pristine $LiCoO_2$ and Al_2O_3, MgO, $MgAl_2O_4$-modified $LiCoO_2$ was evaluated on a LANHE multichannel battery cycler. In a typical activation procedure, all the cells were initially cycled twice between 3.0 and 4.5 V at 0.1C rate (1C = 160 mA g^{-1}). Then the cycling tests were performed at a current rate of 1C in the constant current–constant voltage (CC–CV) charge mode and constant current (CC) discharge mode between 3.0 and 4.5 V. The electrochemical impedance spectra (EIS) of the Li||$LiCoO_2$ cells at the 100% state of charge (SOC) were measured on a CHI 604D electrochemical workstation (Chenhua Instruments Co. Ltd). The frequency range and potential perturbation were set from 100 kHz to 0.01 Hz and 10 mV, respectively.

Results and discussion

Structure and morphology

The XRD patterns of the pristine $LiCoO_2$ and the modified $LiCoO_2$ samples are shown in Fig. 1. From Fig. 1a, all the strong diffraction peaks except the peak at 28.5° (from the internal standard Si) can be indexed to the hexagonal phase with space group $R\bar{3}m$ (JPCDS card no. 50-0653). No diffraction peak corresponding to Al_2O_3, MgO and $MgAl_2O_4$ can be clearly observed in the modified samples owing to their low content of 1%. Even though all the 1% Al_2O_3, MgO and $MgAl_2O_4$ modifications do not greatly affect the crystal structure of $LiCoO_2$, the (003) peak at around 19° displays a distinct shift in every modified $LiCoO_2$ sample in Fig. 1b. The left shift to a smaller degree means the increase of the lattice parameters and the swelling of the lattice

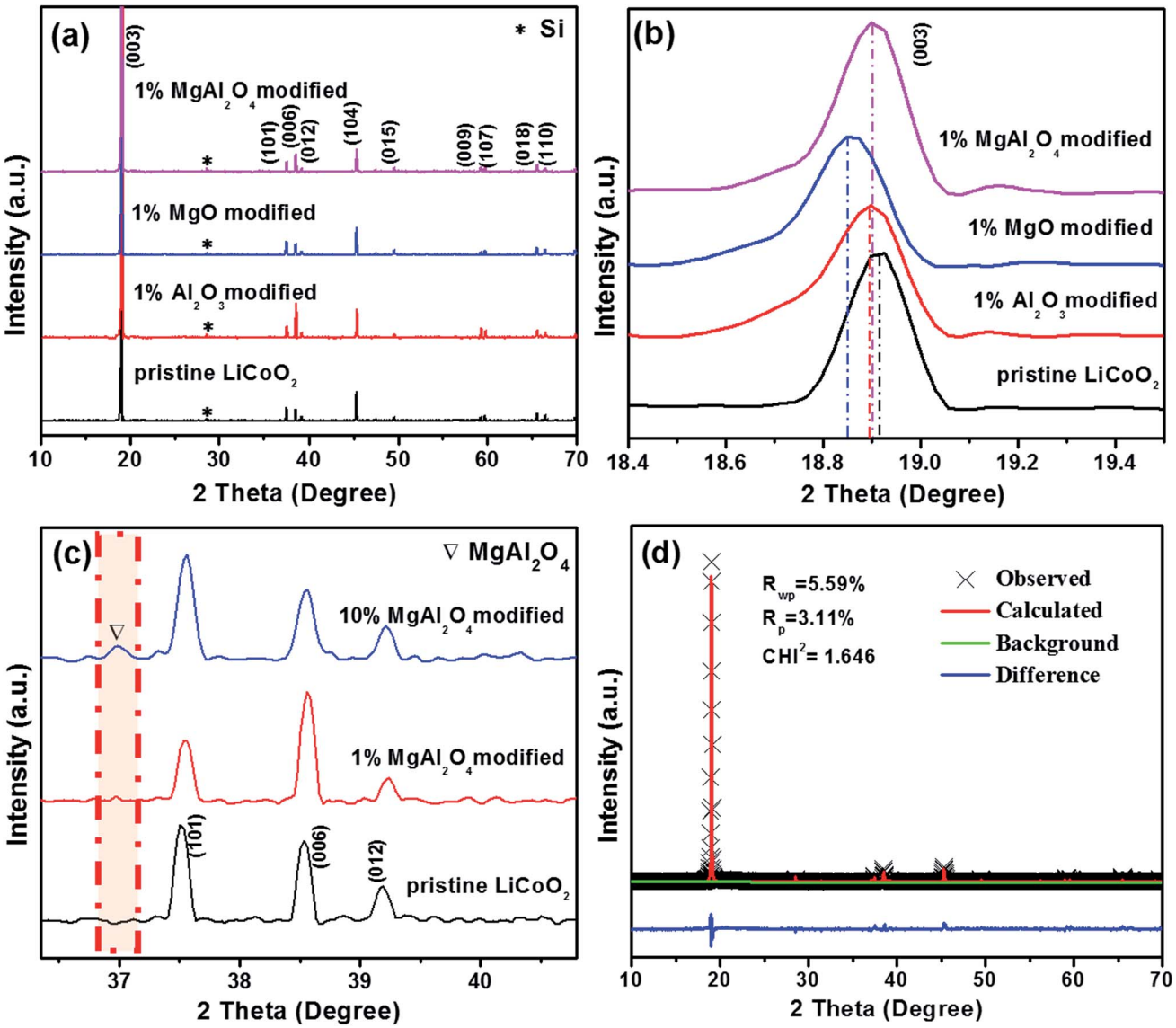

Fig. 1 XRD patterns (a) and magnified (003) peaks (b) of the pristine $LiCoO_2$ and the 1% Al_2O_3, MgO, $MgAl_2O_4$-modified $LiCoO_2$ samples; magnified XRD patterns (c) of the pristine $LiCoO_2$ and 1%, 10% $MgAl_2O_4$-modified $LiCoO_2$ samples; and Rietveld refinement patterns (d) of 1% $MgAl_2O_4$-modified $LiCoO_2$.

volume, which is in agreement with the previous literatures.[7,8] During high-temperature surface modification, Mg^{2+} and Al^{3+} cations could partially dope into the $LiCoO_2$ lattice from the modified layer.[24] Since the ionic size of Al^{3+} (0.535 Å) is smaller than that of Mg^{2+} (0.720 Å), Al^{3+} diffuses into the $LiCoO_2$ lattice more easily than Mg^{2+}. That is the reason for the order of the (003) peak position: MgO modification < $MgAl_2O_4$ modification < Al_2O_3 modification. This is also consistence with mostly recent viewpoint that modification species can be incorporated at grain boundaries into the $LiCoO_2$ surface and lead to reversible structural changes.[14] In order to confirm the formation of spinel $MgAl_2O_4$, Fig. 1c shows the magnified XRD patterns of the 10 wt% $MgAl_2O_4$-modified $LiCoO_2$ sample compared with the pristine and the 1 wt% $MgAl_2O_4$-modified $LiCoO_2$. The full-range XRD patterns can be found in ESI (Fig. S1†), which shows that no peak of $MgAl_2O_4$ is observed due to the low quantity unless the amount increases to 10 wt%. From the magnified XRD patterns in Fig. 1c, the existence of spinel $MgAl_2O_4$ is confirmed by the peak at 37°,[21] which corresponds to the (311) plane of $MgAl_2O_4$ lattice. The Rietveld refinement patterns of the 1% $MgAl_2O_4$-modified $LiCoO_2$ shown in Fig. 1d further prove the existence of spinel $MgAl_2O_4$ in the 1% $MgAl_2O_4$-modified $LiCoO_2$ and the real content of spinel $MgAl_2O_4$ is about 0.6%.

Fig. 2 shows SEM images of the pristine $LiCoO_2$ and 1 wt% Al_2O_3, MgO, $MgAl_2O_4$-modified $LiCoO_2$ samples. The surface of the pristine $LiCoO_2$ (Fig. 2a) is quite smooth and clean, but some stuff can be found on the surfaces of the Al_2O_3, MgO, $MgAl_2O_4$-modified $LiCoO_2$ particles shown in Fig. 2b–d. Quite different from the loose connection between the modified MgO and the $LiCoO_2$ particle (Fig. 2c), the tight connections between the modified Al_2O_3 or $MgAl_2O_4$ with the $LiCoO_2$ particle are

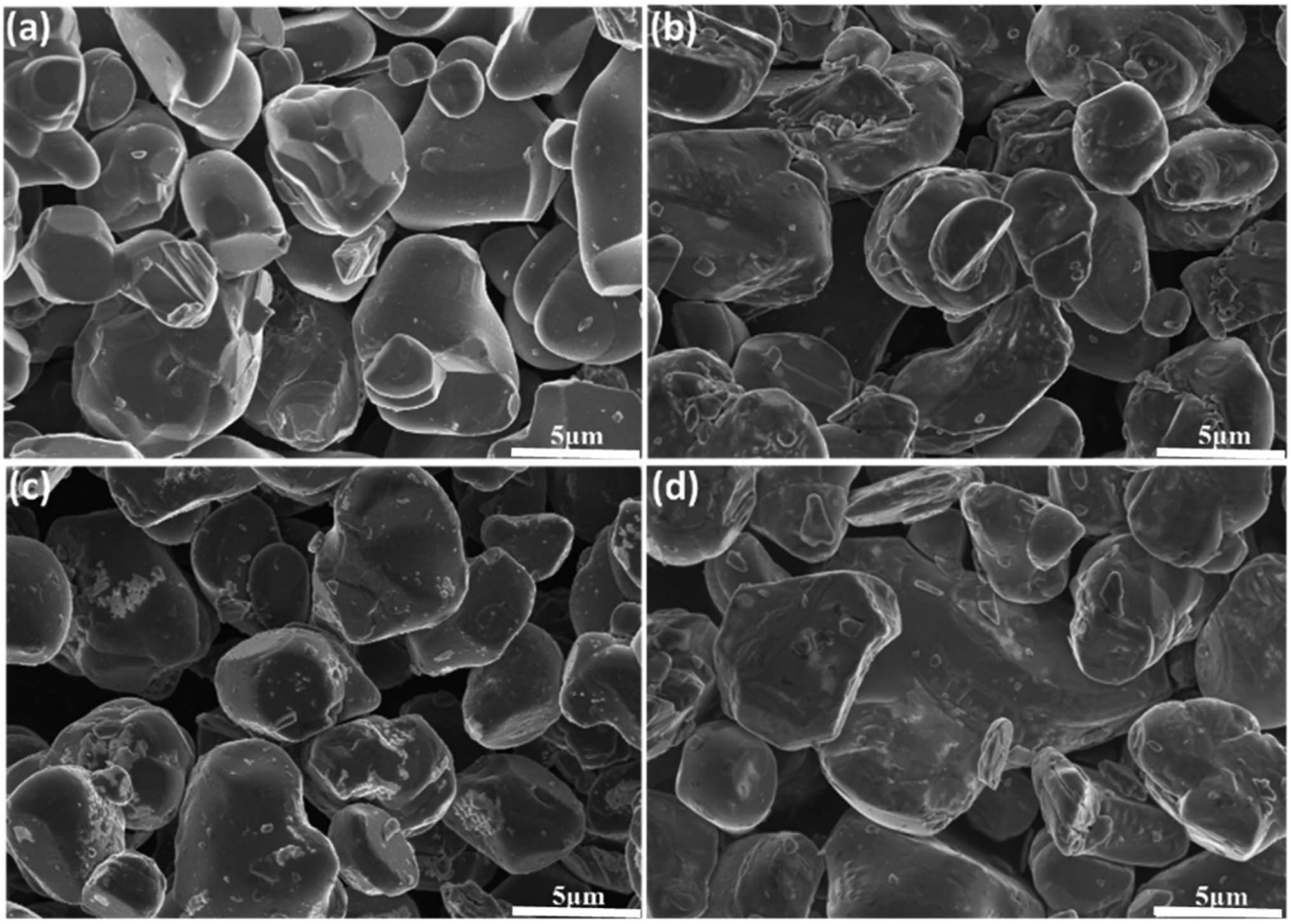

Fig. 2 SEM images of (a) the pristine $LiCoO_2$; (b) Al_2O_3-modified $LiCoO_2$; (c) MgO-modified $LiCoO_2$; (d) and $MgAl_2O_4$-modified $LiCoO_2$ at high magnification (×5.0k).

shown clearly in Fig. 2b and d. Since Al^{3+} ion (0.535 Å) has the smaller size than Mg^{2+} ion (0.720 Å), it is reasonable for more Al^{3+} diffusion from Al_2O_3 and $MgAl_2O_4$ into the $LiCoO_2$ lattice than Mg^{2+} from MgO during the high-temperature treatment, which enhances the connection between the modified material and the $LiCoO_2$ bulk. The tight connection between the modified material and the $LiCoO_2$ bulk means a pretty stable and conformal surface modification. It is indicative of that the Al_2O_3 and $MgAl_2O_4$ modifications have the higher coverage ratios than the MgO modification, and thus more effectively suppress the structural collapse of $LiCoO_2$ and interfacial side reactions between the charged cathode and the electrolyte. In order to check the uniformity of the $MgAl_2O_4$ modification layer, EDS mapping was further performed and the results are shown in Fig. 3. It is clearly shown that the elements O, Al and Mg are uniformly dispersed on the surface of the $MgAl_2O_4$-modified $LiCoO_2$. That means the elements Mg and Al in the $MgAl_2O_4$-modified $LiCoO_2$ sample are uniformly distributed, illustrating that the $MgAl_2O_4$ modification is quite uniform and conformal.

In order to observe the thickness of the surface modification layer in the $MgAl_2O_4$-modified $LiCoO_2$, Fig. 4 shows the HRTEM images of a $MgAl_2O_4$-modified $LiCoO_2$ particle. The modification layer (translucent) has the thickness of around 10 nm and the lattice fringe of *ca.* 0.244 nm is consistent with the interplanar distance of (311) planes of spinel $MgAl_2O_4$. The dark region shows the (006) planes of layered $LiCoO_2$ crystal with the fringe of *ca.* 0.234 nm. Fig. 4 also clearly shows that the modification layer is tightly attached on the surface of $LiCoO_2$, which is beneficial to adequately suppress the interfacial side reactions between the charged $LiCoO_2$ and the electrolyte.

The oxidation states of the Co and O elements in the pristine $LiCoO_2$ and three modified $LiCoO_2$ samples were investigated by XPS as shown in Fig. 5. The Co 2p peaks for the pristine and modified $LiCoO_2$ shown in Fig. 5a included a 2p1/2 peak at around 780 eV and a 2p3/2 peak at around 795 eV.[2] The modified $LiCoO_2$ samples show a shift in the Co 2p1/2 peak by 0.1–0.3 eV toward a higher binding energy than the pristine, which indicates that the Co bonding environment in the surface of the modified samples has a small change.[7] Similar change can also be found in O 1s peaks as shown in Fig. 5b. The O 1s peak at 529.3 eV is assigned to O^{2-} ions in the O_3 layered structure of $LiCoO_2$, and the higher binding energy for the O 1s peak in the modified $LiCoO_2$ samples is attributed to the Al/Mg substitution in Co site on the particle surface.[2] The O 1s peak at 531.3 eV is difficult to be speculated but should be due to the free oxygen/adsorbed oxygen.[25] In the modified $LiCoO_2$ samples, the

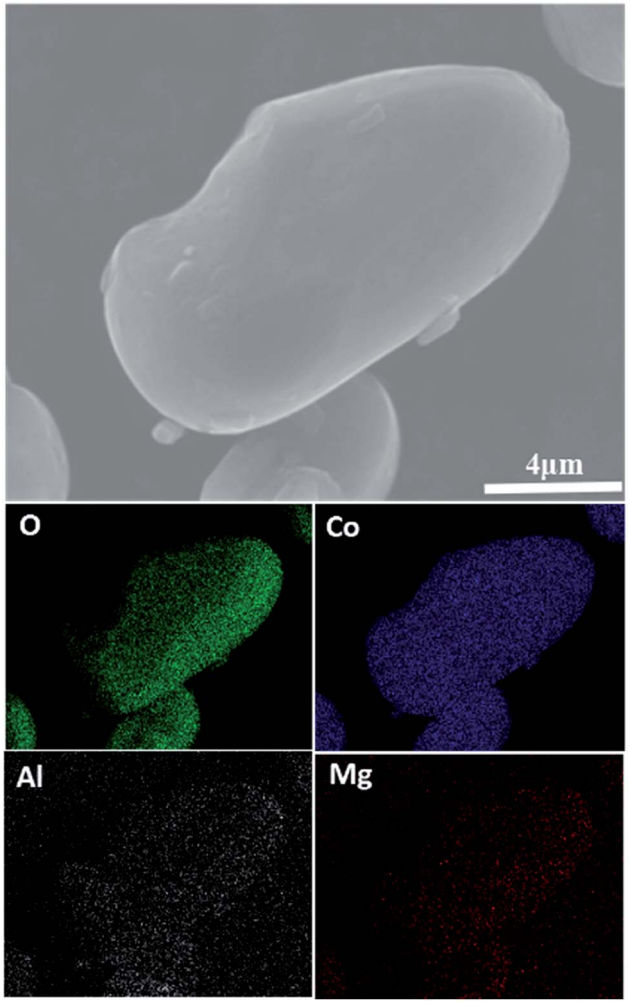

Fig. 3 EDS maps for $MgAl_2O_4$-modified $LiCoO_2$ particles.

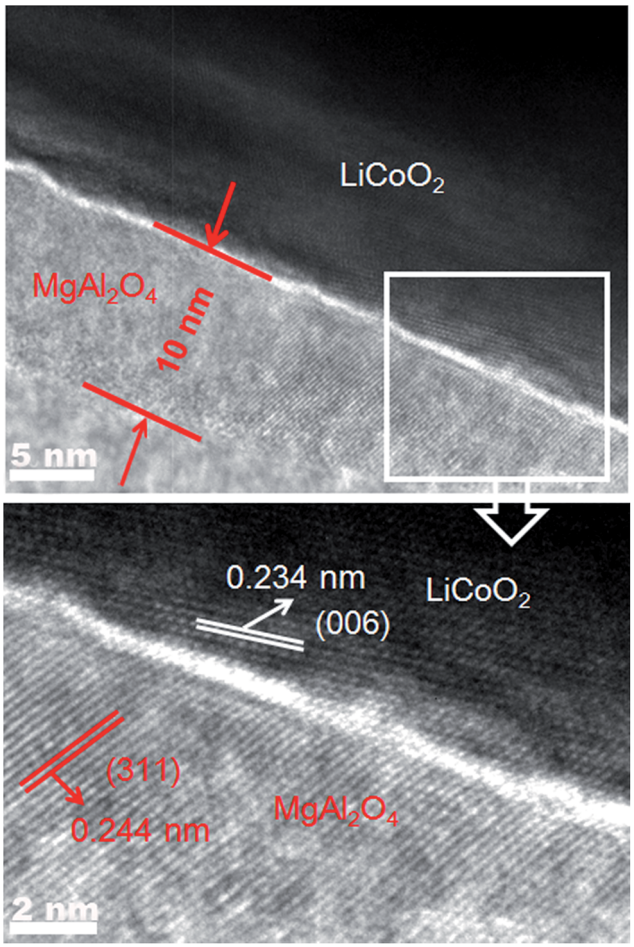

Fig. 4 HRTEM images of a $MgAl_2O_4$-modified $LiCoO_2$ particle.

$MgAl_2O_4$ modification reveals the slight differences on both the Co 2p and O 1s peaks from the Al_2O_3 modification and MgO modification. More interestingly, the lower intensities for the Co 2p peak and the O 1s peak at 531.3 eV for the $MgAl_2O_4$ modified $LiCoO_2$ suggest that the $MgAl_2O_4$ modification is more uniform than the MgO modification, which is accordance with the SEM results shown in Fig. 2. Fig. 5c and d show the depth profiles of Al and Mg elements in the 1% $MgAl_2O_4$-modified $LiCoO_2$. At an etch level of 0 nm, the peak at 73 eV in Fig. 5c is ascribed to the binding energy of Al 2p.[5] The intensity of the Al 2p peak greatly decreases at the level of 10 nm and that peak completely disappeared at the level of 50 nm, which indicates that Al is just present on the surface region of the $MgAl_2O_4$ modified $LiCoO_2$. Similarly as the depth profiles of Al 2p, the intensity of the Mg 2p peak at 49 eV in Fig. 5d[26] drops obviously from the etch level of 0 nm to 10 nm.

Electrochemical properties

Electrochemical properties of the pristine $LiCoO_2$ and Al_2O_3, MgO, $MgAl_2O_4$-modified $LiCoO_2$ were evaluated in the Li|| $LiCoO_2$ coin-cells. Fig. 6 shows initial, 10th, 40th and 70th charge–discharge curves of the pristine $LiCoO_2$ and Al_2O_3, MgO, $MgAl_2O_4$-modified $LiCoO_2$ cells between 3.0 and 4.5 V, respectively. From the initial voltage profiles in Fig. 6a, the pristine and MgO-modified $LiCoO_2$ display slightly higher discharge capacity than the Al_2O_3 and the $MgAl_2O_4$ modified $LiCoO_2$. Moreover, the latter two have higher charge voltage plateau, especially for the Al_2O_3-modified sample, which corresponds to the high electrochemical polarization. Cyclic voltammograms (CVs) results also clearly indicate that the Al_2O_3 and the $MgAl_2O_4$ modified $LiCoO_2$ samples exhibit higher electrochemical polarization in ESI (Fig. S2†). At the 10th cycle (Fig. 6b), the MgO and $MgAl_2O_4$-modified $LiCoO_2$ samples deliver the higher discharge capacities than the pristine and the Al_2O_3-modified $LiCoO_2$ samples. However, the pristine $LiCoO_2$ shows both fast capacity fading and voltage fading at the 40th cycle (Fig. 6c), which is just similar as previous literatures.[3,6,27] Different from the Al_2O_3 and $MgAl_2O_4$-modified $LiCoO_2$, the MgO-modified $LiCoO_2$ experiences a visible capacity fading from 180 mA h g^{-1} at the 10th cycle to 160 mA h g^{-1} at the 40th cycle. Furthermore, at the 70th cycle shown in Fig. 6d, the MgO-modified $LiCoO_2$ exhibits a serious capacity fading to 120 mA h g^{-1}, along with a big voltage plateau drop. The $MgAl_2O_4$-modified $LiCoO_2$ shows higher capacity than the others at the 70th

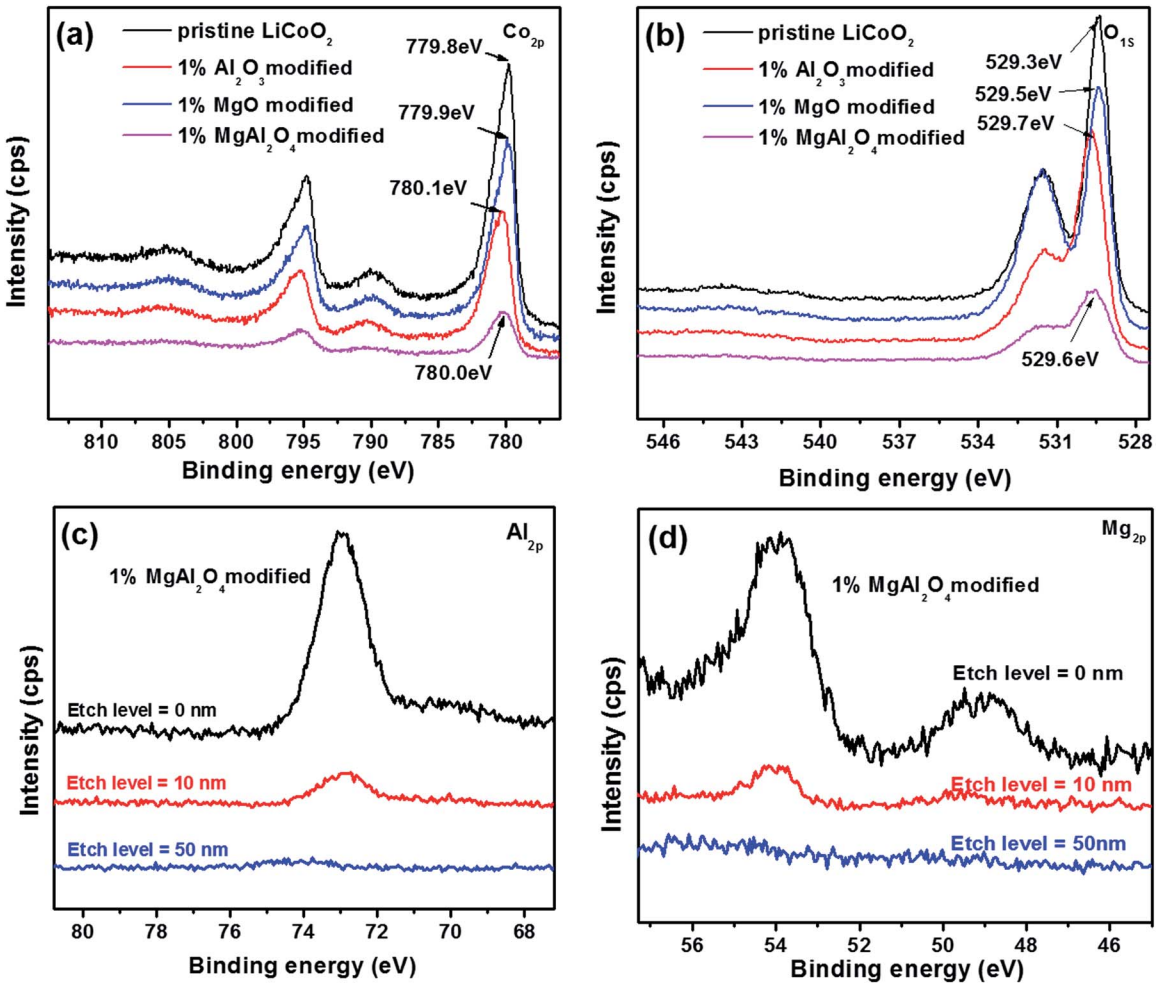

Fig. 5 XPS spectra (a, b) of the pristine $LiCoO_2$ and Al_2O_3, MgO, $MgAl_2O_4$-modified $LiCoO_2$ samples, and the depth profiles of Al (c) and Mg (d) elements in the 1% $MgAl_2O_4$-modified $LiCoO_2$.

cycle. The cycling performance of the pristine $LiCoO_2$ and Al_2O_3, MgO, $MgAl_2O_4$-modified $LiCoO_2$ was shown in Fig. 7. Clearly, the discharge capacity of the pristine $LiCoO_2$ drops to 72 mA h g^{-1} after 70 cycles, with the capacity retention of 42% (*vs.* the capacity of the 3rd cycle). Although the MgO-modified $LiCoO_2$ has the higher discharge capacity at the first twenty cycles than the others, a fast capacity fading leads to the capacity of only 115 mA h g^{-1} after 70 cycles with the capacity retention of 63%. Herein, the MgO modification can improve the capacity but has invisible effect on enhancing the cycling stability, which is in accordance with the Shim's result.[8] However, both the Al_2O_3 and $MgAl_2O_4$-modified $LiCoO_2$ samples show the excellent cycling stability with the capacity retention over 96% after 70 cycles. Especially, the $MgAl_2O_4$-modified $LiCoO_2$ has not only the excellent cycling stability and also the highest capacity. The enhanced electrochemical performance of the $MgAl_2O_4$-modified $LiCoO_2$ is mainly attributed to both the uniform modification layer (Fig. 2d) and Mg^{2+}/Al^{3+} dopings on the surface of $LiCoO_2$ particles (Fig. 1b). The uniform $MgAl_2O_4$ layer can effectively prevent the oxidation decomposition of the electrolyte and Co^{4+} dissolution into the electrolyte at high voltages.[6,8] These results clearly indicate that the $MgAl_2O_4$ modification exhibits the combined advantages of the Al_2O_3 modification on cycling stability and the MgO modification on capacity improvement. In addition, in our study the 1% $MgAl_2O_4$ modification is better than 0.5% and 2% modification (Fig. S3 in ESI†). The optimal composition of $MgAl_2O_4$ means the appropriate thickness of the modification layer. It is vital to not only provide vigorous protection for $LiCoO_2$ from the electrolyte corrosion (resulting in Co^{4+} dissolution), but also allow Li^+ ion transport fluently (lower impedance).

Fig. 8 shows rate capabilities of the pristine $LiCoO_2$ and Al_2O_3, MgO, $MgAl_2O_4$-modified $LiCoO_2$ samples between 3.0 and 4.5 V. After two formation cycles at 0.1C, all the cells were charged at a rate of 0.5C and discharged at incremental rates from 0.5 to 5C followed by recovering back to 0.5C. In the case of the pristine $LiCoO_2$, its discharge capacity rapidly drops with increasing the current rates and even at the same rate the capacity fades fast, just similar as the cycling performance shown in Fig. 7. The three modified $LiCoO_2$ samples exhibit the enhanced rate capability, presumably due to the positive effect of Mg^{2+}/Al^{3+} surface dopings on increasing ionic conductivity.

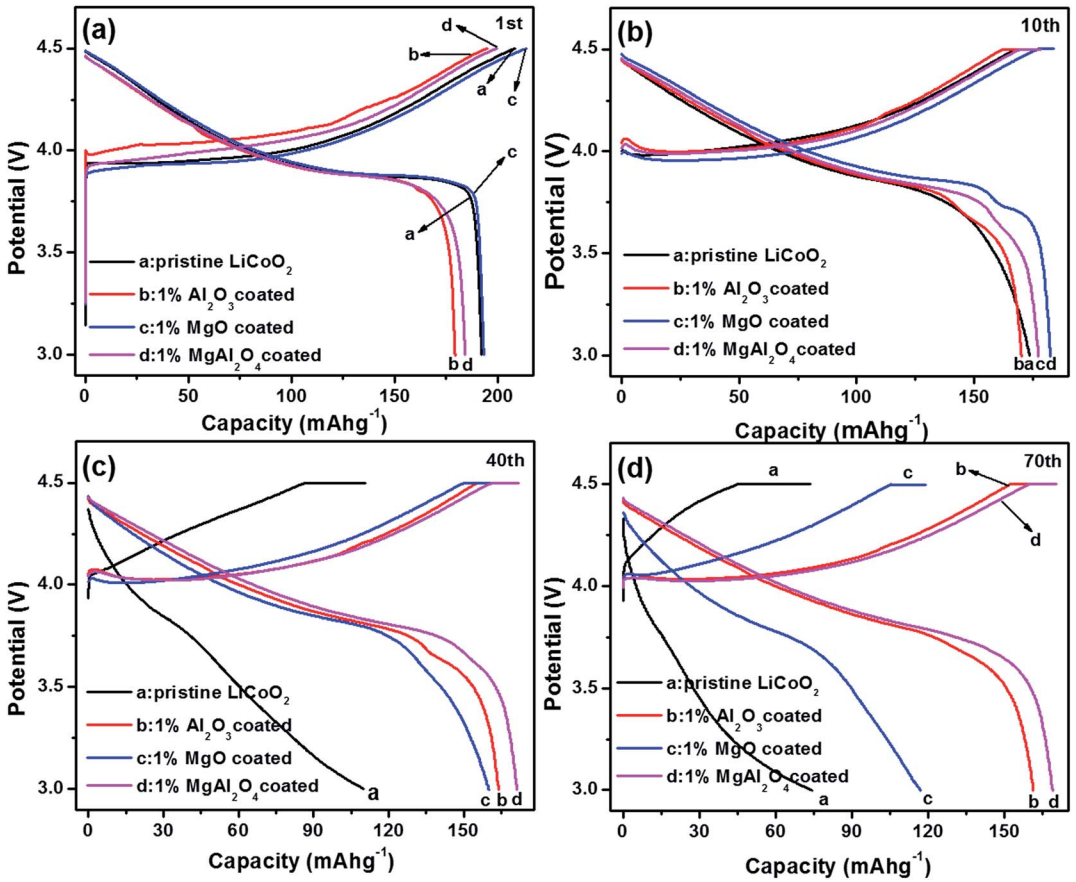

Fig. 6 Charge and discharge curves of the pristine $LiCoO_2$ and Al_2O_3, MgO, $MgAl_2O_4$-modified $LiCoO_2$ at (a) the first cycle; (b) the 10th cycle; (c) the 40th cycle and (d) the 70th cycle.

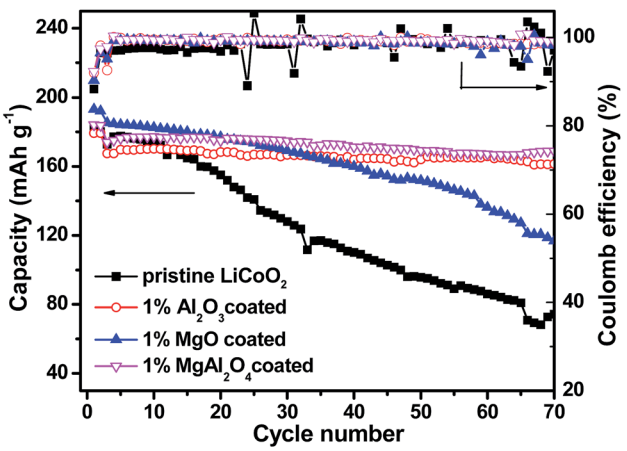

Fig. 7 Cycling performance at the current rate of 1C and coulombic efficiency of the pristine $LiCoO_2$ and Al_2O_3, MgO, $MgAl_2O_4$-modified $LiCoO_2$.

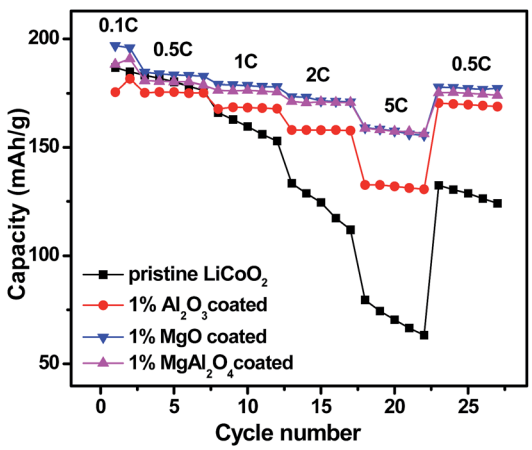

Fig. 8 Rate capability of the pristine the pristine $LiCoO_2$ and Al_2O_3, MgO, $MgAl_2O_4$-modified $LiCoO_2$.

The Al_2O_3-modified $LiCoO_2$ delivers the capacities of 168 mA h g^{-1} at 1C, 157 mA h g^{-1} at 2C and 133 mA h g^{-1} at 5C. Similar as their higher capacities shown in Fig. 7, the MgO and $MgAl_2O_4$-modified $LiCoO_2$ samples show higher rate capabilities than the Al_2O_3-modified $LiCoO_2$. Both the MgO and $MgAl_2O_4$-modified $LiCoO_2$ samples deliver the capacity of 158 mA h g^{-1} at 5C. In addition, when the current rate returns back to 0.5C, the discharge capacities of all the modified samples can be restored. The enhanced rate capability of the $MgAl_2O_4$-modified $LiCoO_2$ is possibly due to high Li^+ ion conductivity of the $MgAl_2O_4$ layer.

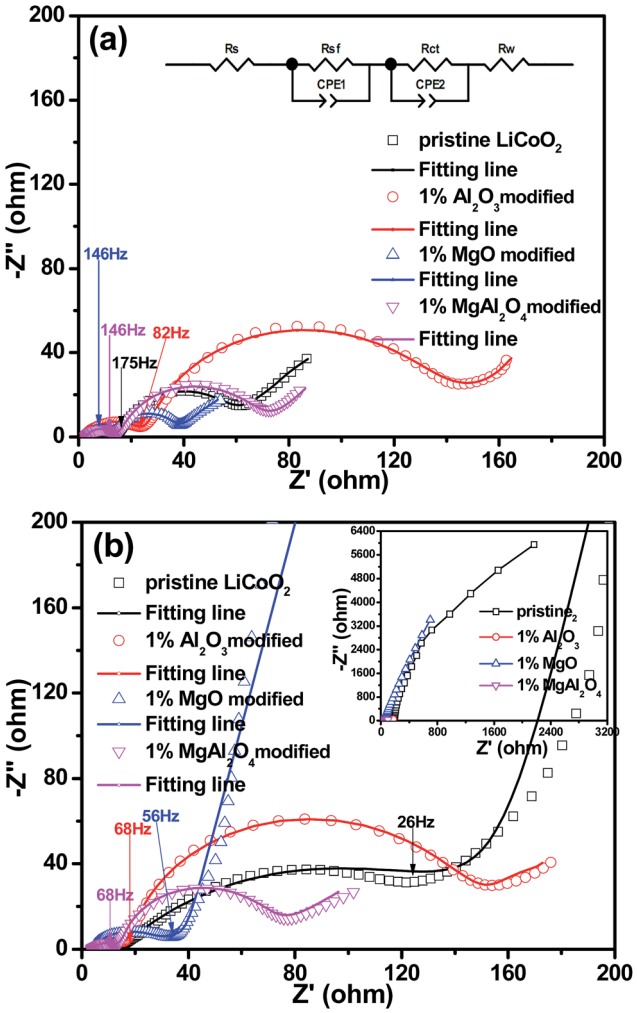

Fig. 9 Electrochemical impedance spectra (EIS) of the pristine $LiCoO_2$ and Al_2O_3, MgO, $MgAl_2O_4$-modified $LiCoO_2$ at full discharge (a) after 2 cycles; (b) after 70 cycles.

To further understand the effect of the $MgAl_2O_4$ modification on the electrochemical performance of $LiCoO_2$, EIS results of the Li||$LiCoO_2$ cells using the pristine $LiCoO_2$ and Al_2O_3, MgO, $MgAl_2O_4$-modified $LiCoO_2$ materials are compared in Fig. 9. The Nyquist plots of the cells after 2 cycles (Fig. 9a) and 70 cycles (Fig. 9b) are composed of two semicircles in the high-to-medium frequency range and an inclined line in the low frequency range, similar as previously reported.[11,13,28–30] The inset equivalent circuit in Fig. 9a is used to fit the Nyquist plots. The semicircle in the high frequency range (>20 Hz) can reflect the impedance (R_{sf}) for Li^+ ion migration through the solid-electrolyte interphase (SEI) films which occur both on the cathode and Li anode,[31,32] where the frequencies are shown as labelled. Considering that the same electrolyte and highly-purity Li metal were used, the differences on the SEI film impedances are attributed to the different $LiCoO_2$ cathodes. The semicircle in the medium frequency range and the inclined line represent the charge transfer impedance (R_{ct}) and the Warburg impedance (W), respectively. In Fig. 9a, the Al_2O_3-modified $LiCoO_2$ exhibits the higher interface impedance than the pristine $LiCoO_2$, which is consistent with previous literatures.[6] However, both the MgO and $MgAl_2O_4$-modified $LiCoO_2$ samples have the slightly smaller interface impedance than the pristine $LiCoO_2$. The difference on the interface impedances is one of the main reasons for the difference on the capacity of the modified or unmodified $LiCoO_2$ cathode materials, as proposed previously.[3,29] After 70 cycles (Fig. 9b), the Al_2O_3 and $MgAl_2O_4$-modified $LiCoO_2$ samples experience negligible increases on the interface impedance as well as the charge transfer impedance. These results strongly suggest that both the Al_2O_3 and $MgAl_2O_4$ modifications are so stable that the oxidation decomposition of the electrolyte on the charged $LiCoO_2$ can be effectively suppressed and the structure of $LiCoO_2$ bulk keeps stable. However, the MgO-modified $LiCoO_2$ shows a distinct increase on interface impedance, even though its increase is not as rapid as that of the pristine $LiCoO_2$. Moreover, the full plot parts of the pristine and the MgO-modified $LiCoO_2$ samples in the inset of Fig. 9b (the region with low impedance values) mean much higher charge transfer impedances than the Al_2O_3 and $MgAl_2O_4$-modified $LiCoO_2$ samples. That means the MgO surface modification could not essentially stabilize the surface structure of the $LiCoO_2$ against the electrolyte at high-voltage cycling. Herein, the charge transfer impedances are not discussed. Nevertheless, the change on the interface impedances of various $LiCoO_2$ samples are in consonance with their cycling stabilities shown in Fig. 7. In summary, the $MgAl_2O_4$ modification has the combined advantages on the high conductivity of the MgO modification and excellent stability of the Al_2O_3 modification.

Conclusions

Spinel $MgAl_2O_4$ modification has been successfully carried out on the surface of $LiCoO_2$ cathode material, and the modification layer is conformal and fairly uniform. The $MgAl_2O_4$ modification layer shows the positive effects of combining the Al_2O_3 modification on the cycling stability and the MgO modification on the conductivity. Therefore, the $MgAl_2O_4$-modified $LiCoO_2$ exhibits excellent cycling stability and rate capability at high voltages up to 4.5 V. Such results indicate that the $MgAl_2O_4$ spinel is a good modification material for $LiCoO_2$ cathode for high-voltage Li ion batteries.

Acknowledgements

This study was supported by National Science Foundation of China (Grant No. 51372060 and 21676067) and the Opening Project of CAS Key Laboratory of Materials for Energy Conversion (KF2016005).

Notes and references

1 M. S. Whittingham, *Chem. Rev.*, 2004, **104**, 4271.
2 A. T. Appapillai, A. N. Mansour, J. Cho and S.-H. Yang, *Chem. Mater.*, 2007, **19**, 5748.
3 Y. Kim, G. M. Veith, J. Nanda, R. R. Unocic, M. F. Chi and N. J. Dudney, *Electrochim. Acta*, 2011, **56**, 6573.

4 H. Miyashiro, Y. Kobayashi, S. Seki, Y. Mita, A. Usami, M. Nakayama and M. Wakihara, *Chem. Mater.*, 2005, **17**, 5603.
5 G. T. K. Fey, H. M. Kao, P. Muralidharan, T. P. Kumar and Y. D. Cho, *J. Power Sources*, 2006, **163**, 135.
6 F. Zhao, Y. Tang, J. Wang, J. Tian, H. Ge and B. Wang, *Electrochim. Acta*, 2015, **174**, 384.
7 M. Xie, T. Hu, L. Yang and Y. Zhou, *RSC Adv.*, 2016, **6**, 63250.
8 J.-H. Shim, S. Lee and S. S. Park, *Chem. Mater.*, 2014, **26**, 2537.
9 Y. Iriyam, H. Kurita, I. Yamada, T. Abe and Z. Ogumi, *J. Power Sources*, 2004, **137**, 111.
10 G. Q. Liu, H. T. Kuo, R. S. Liu, C. H. Shen, D. S. Shy, X. K. Xing and J. M. Chen, *J. Alloys Compd.*, 2010, **496**, 512.
11 B. J. Hwang, C. Y. Chen, M. Y. Cheng, R. Santhanam and K. Ragavendran, *J. Power Sources*, 2010, **195**, 4255.
12 J. Cho, C. Kim and S. I. Yoo, *Electrochem. Solid-State Lett.*, 2000, **3**, 362.
13 J. Cho, Y. J. Kim and B. Park, *Angew. Chem., Int. Ed.*, 2001, **40**, 3367.
14 S. Taminato, M. Hirayama, K. Suzuki, K. Tamura, T. Minato, H. Arai, Y. Uchimoto, Z. Ogumi and R. Kanno, *J. Power Sources*, 2016, **307**, 599.
15 D. Takamatsu, S. Mori, Y. Orikasa, T. Nakatsutsumi, Y. Koyama, H. Tanida, H. Arai, Y. Uchimoto and Z. Ogumi, *J. Electrochem. Soc.*, 2013, **160**(5), A3054.
16 L. L. Zhang, J. J. Chen, S. Cheng and H. F. Xiang, *Ceram. Int.*, 2016, **42**, 1870.
17 A. Zhou, J. Xu, X. Dai, B. Yang, Y. Lu, L. Wang, C. Fan and J. Li, *J. Power Sources*, 2016, **322**, 10.
18 X. Pu and C. Yu, *Nanoscale*, 2012, **4**, 6743.
19 M. J. Mees, G. Pourtois, F. Rosciano, B. Put, P. M. Vereecken and A. Stesmans, *Phys. Chem. Chem. Phys.*, 2014, **16**, 5399.
20 R. Djenadic, M. Botros and H. Hahn, *Solid State Ionics*, 2016, **287**, 71.
21 N. Angulakshmi, K. S. Nahm, J. R. Nair, C. Gerbaldi, R. Bongiovanni and N. Penazzi, *Electrochim. Acta*, 2013, **90**, 179.
22 N. Ozawa, K. Donoue and T. Yao, *Electrochem. Solid-State Lett.*, 2003, **6**, A106.
23 G. T. K. Fey, Z.-F. Wang, C.-Z. Lu and T. P. Kumar, *J. Power Sources*, 2005, **146**, 245.
24 C. Li, H. P. Zhang, L. J. Fu, H. Liu, Y. P. Wu, E. Rahm, R. Holze and H. Q. Wu, *Electrochim. Acta*, 2006, **51**, 3872.
25 G. Chen, H. Geng, Z. Wang, R. Yang and Y. Xu, *Ionics*, 2016, **22**, 629.
26 S. J. Shi, J. P. Tu, Y. Y. Tang, X. Y. Liu, Y. Q. Zhang, X. L. Wang and C. D. Gu, *Electrochim. Acta*, 2013, **88**, 671.
27 K. C. Kim, J.-P. Jegal, S.-M. Bak, K. C. Roh and K.-B. Kim, *Electrochem. Commun.*, 2014, **43**, 113.
28 G. R. Hu, J. C. Cao, Z. D. Peng, Y. B. Cao and K. Du, *Electrochim. Acta*, 2014, **149**, 49.
29 B. Wu, Y. Ren, D. Mu, X. Liu, G. Yang and F. Wu, *RSC Adv.*, 2014, **4**, 10196.
30 J. Zhang, Y. J. Xiang, Y. Yu, S. Xie, G. S. Jiang and C. H. Chen, *J. Power Sources*, 2004, **132**, 187.
31 C. H. Chen, J. Liu and K. Amine, *J. Power Sources*, 2001, **96**, 321–328.
32 A. Sakuda, A. Hayashi and M. Tatsumisago, *J. Power Sources*, 2010, **195**, 599.